Identification of Oxidation Products in Selectively Labeled Polypropylene with Solid-State ^{13}C NMR Techniques

Daniel M. Mowery,*,† Roger L. Clough, and Roger A. Assink

Organic Materials Department, Sandia National Laboratories, Albuquerque, New Mexico 87185

Received November 22, 2006; Revised Manuscript Received January 7, 2007

ABSTRACT: Oxidatively degraded polypropylene (PP) samples, with selective ^{13}C labeling of the three carbon sites on the PP chain (tertiary, secondary, and methyl carbons), have been analyzed with a suite of one- and two-dimensional solid-state ^{13}C nuclear magnetic resonance (NMR) experiments that have been used to assign several ^{13}C resonances attributed to oxidation-induced functional groups. These NMR techniques, several of which were recently developed, included dipolar dephasing for MAS speeds ≥10 kHz, chemical shift anisotropy (CSA) filtering, SUPER NMR to separate quasi-static CSA patterns, and $^{1}H-^{13}C$ heteronuclear correlation (HETCOR). In the course of the study, it has been demonstrated that NMR experiments which utilize the ^{13}C CSA for resonance identification can be sensitive to sample temperature as a result of molecular motion-induced averaging of the CSA. These experiments have allowed hemiketal groups to be identified for the first time to our knowledge in oxidized PP. Possible mechanisms for the formation of hemiketals and other functional groups have been discussed.

1. Introduction

Synthetic hydrocarbon polymers such as polypropylene (PP) are susceptible to oxidative degradation initiated by environmental stresses such as heat, ultraviolet radiation, and γ radiation. An understanding of the underlying mechanisms of oxidation in these materials is critical in developing more effective antioxidant systems and altering chain microstructure to improve material lifetime and durability. An integral component in discerning and, subsequently, modeling oxidation chemistry is the identification of chemical species, both stable and intermediate, that are formed during oxidation. Many of the products formed in polypropylene subjected to long-term oxidative degradation have been identified,[1,2] while others are in question or have yet to be realized. For example, in earlier solution-state ^{13}C NMR studies[3,4] of oxidatively degraded polypropylene, a ^{13}C resonance was observed near 112 ppm. On the basis of the isotropic chemical shift alone, this resonance could be assigned to either the vinylidene group (CH_2═CH−), an unsaturated structure, or to dioxygenated alkyl structures (O−C−O), such as acetal and ketal groups. Such a distinction is important, as different oxidation pathways and structural changes in the degrading polymer could have significantly different effects on the material properties (e.g., chain scission vs cross-linking). The researchers[3,4] in these previous NMR studies identified the peak with the vinylidene group.

We have utilized selective ^{13}C isotopic labeling of polypropylene in combination with solid-state ^{13}C nuclear magnetic resonance (NMR) spectroscopy[5,6] and GC−mass spectroscopy[7,8] to analyze the oxidative degradation of polypropylene. By selectively labeling the three carbon sites on the PP chain (tertiary, secondary, and methyl carbons), we are able to more effectively discern chemical pathways in polypropylene oxidation by tracing the oxidation products to their origin on the PP chain. Also, ^{13}C labeling increases signal sensitivity by 2 orders of magnitude, making solid-state NMR measurements more accessible. Given the low thermal stability expected for many of the PP oxidation products (such as peroxidic species), direct measurements on the solid samples are more likely to give an accurate picture of the product distribution formed in solid-phase degradation. In solution-state NMR measurements of degraded polypropylene, sample dissolution requires high temperatures (>100 °C) in organic solvents. Hence, the elevated sample temperatures and increased macromolecular mobility resulting from dissolution could induce further chemical reactions that could significantly alter the structure and concentration of the solid-phase oxidation products. Also, some oxidation-induced functional groups could be present in insoluble domains and may not be detected in solution-state measurements because of decreased segmental mobility.

With the increased signal sensitivity and selective ^{13}C labeling, we have obtained kinetic accumulation data and concentration distributions for PP solid-phase oxidation products formed during elevated temperature exposure, γ-irradiation, and postirradiation degradation[5,6] as well as detecting and understanding the origin of major gaseous products.[7,8] However, in our previous solid-state NMR studies[5,6] of oxidatively degraded polypropylene, we have observed several ^{13}C resonances which can be assigned to a number of possible functional groups on the basis of isotropic chemical shifts alone, including the peak near 112 ppm mentioned above. The identification of these resonances is important in developing a more accurate understanding of the long-term oxidation mechanism in polypropylene.

In this paper we apply a suite of advanced solid-state ^{13}C NMR techniques, several of which have been recently developed, to assign and identify several ^{13}C resonances attributed to oxidation-induced functional groups in polypropylene. Our studies have identified hemiketal groups for the first time to our knowledge in oxidatively degraded polypropylene. Mechanisms for the formation of hemiketals and other functional groups are proposed.

2. Experimental Section

2.1. Materials. The current study employed three different polypropylene (PP) materials selectively labeled with the ^{13}C isotope. These materials have been used in a series of recently

* To whom correspondence should be addressed: e-mail MMowery@dow.com; Tel 979-238-1664; Fax 979-238-0752.

† Current address: The Dow Chemical Company, Analytical Sciences R&D Support, 2301 N. Brazosport Blvd., B-1219, Freeport, TX 77541.

10.1021/ma062689j CCC: $37.00
Published on Web 04/21/2007

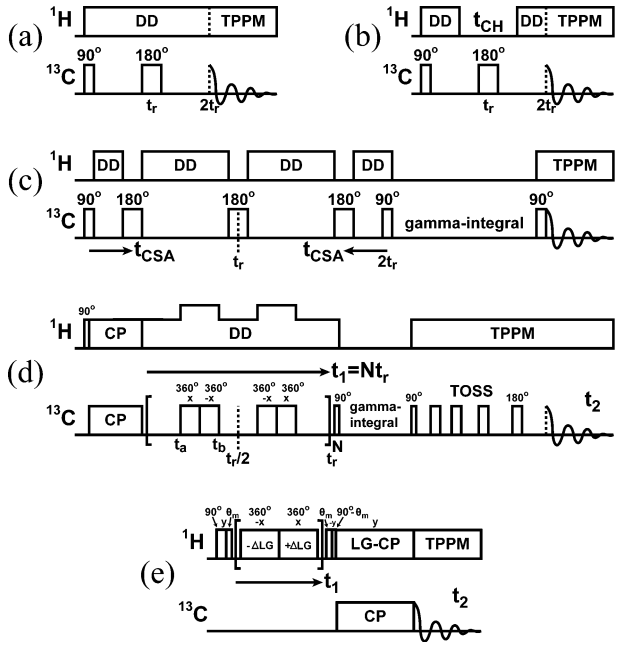

Figure 1. Solid-state ^{13}C NMR pulse sequences used in the current study: (a) DP/MAS pulse sequence to avoid baseline dephasing and distortion,[10] with a ^{13}C 180° pulse after a sample rotation period t_r to form a Hahn echo at $2t_r$; (b) DP/MAS pulse sequence to retain nonprotonated and methyl carbon signals,[10] using C−H dipolar dephasing with recoupling at MAS frequencies ≥10 kHz; (c) DP/MAS with the five-pulse CSA-filtering sequence of Mao and Schmidt-Rohr[11] that selects the signals of sp^3-hybridized carbons while suppressing signals from sp^2- and sp-hybridized carbons; (d) 2D SUPER pulse sequence[13] that recouples the ^{13}C CSA during the evolution time t_1, separating quasi-static CSA patterns in the indirect dimension ω_1 by isotropic ^{13}C chemical shifts in ω_2; (e) $^1H-^{13}C$ heteronuclear correlation (HETCOR) with FS-LG decoupling[15] during t_1 and LG-CP,[16,17] where θ_m is the magic-angle ^1H pulse. DD: C−H dipolar decoupling by continuous-wave irradiation of ^1H. TPPM: C−H dipolar decoupling by two-pulse phase modulation.[9] TOSS: total sideband suppression.[14]

published studies from our laboratory.[5−8] The materials each have distinct labeling schemes of the PP main-chain carbons (tertiary CH, secondary CH_2, and methyl CH_3) and are referred to herein, as in our previous studies, as C(1), C(1,3), and C(2) labeled samples. In the C(2) labeled PP material, the tertiary (or methine) carbons were enriched with ∼99% ^{13}C. In C(1,3) labeled samples, the secondary (or methylene) and primary (or methyl) carbons were enriched with ∼68% and ∼31% ^{13}C. The C(1) labeled PP material was enriched with ∼97% ^{13}C at the secondary carbon site. Further details about the syntheses and properties of these materials can be found elsewhere.[5]

Unstabilized thin films were melt-pressed from the original PP powders, yielding semicrystalline morphologies. These film samples were subsequently exposed to long-term, thermal aging in air, as described in detail in a previous paper.[5] The specific oxidatively aged PP samples selected for analysis in the current study were chosen for their relatively high concentrations of relevant oxidation products, yielding more intense NMR signals of these products.

2.2. NMR Parameters. Solid-state ^{13}C NMR experiments were performed using a Bruker Avance NMR spectrometer operating at a ^{13}C resonance frequency of 100.6 MHz (static field $B_0 = 9.4$ T). A 4 mm magic-angle spinning (MAS) X−H probe head with variable-temperature (VT) capabilities was employed. Zirconia MAS rotors (4 mm o.d.) with Kel-F caps were used. High-power ^1H decoupling at $\gamma B_{1,H}/2\pi = 63$ kHz utilizing the two-pulse phase modulation (TPPM) decoupling scheme[9] was applied during data acquisition in all experiments. The solid-state ^{13}C NMR pulse sequences utilized throughout the current study are presented in Figure 1. ^{13}C direct polarization (DP) based experiments (Figure 1a−c) were acquired with a 60 s recycle delay and a ^{13}C excitation (90°) pulse length of 4 μs. $^{13}C\{^1H\}$ cross-polarization (CP) based experiments (Figure 1d,e) were performed with a 5 s recycle delay. CP contact times varied with the experiment. ^{13}C isotropic chemical shifts were calibrated on the carbonyl resonance of an external glycine standard, +176.0 ppm with respect to TMS (0.0 ppm).

2.2.1. $^{13}C-^1H$ Dipolar Dephasing. In DP experiments with C−H dipolar dephasing and 10 kHz MAS,[10] both a reference spectrum (acquired with the pulse sequence in Figure 1a) and a dipolar-dephased spectrum (Figure 1b) were obtained with the same number of scans (768 or 1024) for each sample analyzed. The ^{13}C 180° refocusing pulse was 8 μs in duration. The 10 kHz MAS frequency was used in our previous NMR work[5,6] and corresponds to a sample rotation period $t_r = 100$ μs. A corresponding C−H dephasing delay $t_{CH} = 94$ μs was employed (Figure 1b). Continuous-wave dipolar decoupling (DD) at $\gamma B_{1,H}/2\pi = 63$ kHz was applied at appropriate times, as shown in Figure 1a,b.

2.2.2. ^{13}C CSA Filtering. DP/MAS spectra with ^{13}C CSA (chemical shift anisotropy) filtering were acquired using the five-pulse sequence of Mao and Schmidt-Rohr,[11] as shown in Figure 1c. A reference spectrum and a CSA-filtered spectrum were obtained for each sample analyzed using the same number of scans (768 or 1024). MAS frequencies of 4 or 5 kHz (corresponding to $t_r = 250$ or 200 μs, respectively) were employed. On the basis of the static field strength ($B_0 = 9.4$ T) and the MAS frequency ($\nu_r =$ 4−5 kHz), a CSA-dephasing delay $t_{CSA} = 35$ μs was used for the CSA-filtered spectrum. The reference spectrum was acquired with $t_{CSA} = 3$ μs. A "γ-integral",[12] a z-dephasing period of ∼1 ms duration that is incremented by $t_r/4$ periods in four consecutive scans, was utilized after the CSA filter and before detection (Figure 1c) to prevent phase-distorted spinning sidebands. The ^{13}C 180° pulse length was 8 μs, and the dipolar decoupling (DD) power was 63 kHz.

2.2.3. 2D SUPER. Quasi-static ^{13}C CSA patterns were obtained using SUPER NMR[13] (pulse sequence in Figure 1d). 2D SUPER spectra were acquired with a 2 ms Hartmann−Hahn CP pulse ($\gamma B_{1,CP}/2\pi = 63$ kHz) preceded by a 4 μs preparation (90°) pulse on ^1H. The recommended CSA scaling factor $\chi' = 0.155$ was utilized. With this scaling factor, the appropriate timings t_a and t_b of the ^{13}C 360° pulses during t_1 (Figure 1d), as well as the ^{13}C field strengths $\gamma_C B_{1,C}/2\pi$ of the 360° pulses, have been calculated.[13] MAS frequencies of 2.5 and 5 kHz were used for alkyl and carbonyl carbons, respectively. The sweep width in ω_1 is proportional to the MAS frequency. Unscaled quasi-static chemical shifts in ω_1 were acquired with a dwell time in t_1 multiplied by 0.155. The number of t_1 increments was 32−64, with 128−256 scans averaged per increment. Dipolar decoupling (DD) at $\gamma B_{1,H}/2\pi = 30$ and 75 kHz was applied between and during the ^{13}C pulses in t_1, respectively (Figure 1d). The γ-integral[12] and the total sideband suppression (TOSS) sequence[14] were applied after the t_1 evolution time and before detection (Figure 1d).

2.2.4. 2D HETCOR. Correlation between ^{13}C and ^1H isotropic chemical shifts was obtained with a solid-state $^1H-^{13}C$ HETCOR experiment (Figure 1e). Homonuclear $^1H-^1H$ couplings were attenuated during the t_1 evolution time using frequency-switched Lee−Goldburg (FS-LG) decoupling[15] at $\gamma B_{1,H}/2\pi = 63$ kHz. Lee−Goldburg CP[16,17] was utilized for the suppression of $^1H-^1H$ spin diffusion during $^1H \rightarrow {}^{13}C$ polarization transfer. The CP contact pulse was 0.5 ms with $\gamma B_{1,CP}/2\pi = 63$ kHz. A 10 kHz MAS speed was used. The HETCOR data presented in this study were the sum of four 2D spectra to enhance resolution of the oxidation-induced functional group resonances in the ^1H dimension by reducing noise. Each 2D HETCOR spectrum was acquired with 128 t_1 increments of 64 μs duration and 128 scans per increment.

3. Results and Discussion

3.1. NMR Approach. In our previous solid-state ^{13}C NMR studies[5,6] probing the long-term oxidative degradation of selectively labeled polypropylene, several ^{13}C resonances attributed to oxidation-induced functional groups were observed. It is the intention of this current work to either confirm or clarify the assignments of these resonances by utilizing a collection of

1D and 2D solid-state ^{13}C NMR techniques (Figure 1). These techniques were recently employed in the characterization of biosolids-derived organic matter[18] and natural organic material (such as organic components found in soil samples).[10,11] In the ^{13}C NMR spectra of such organic matter, as in oxidized hydrocarbon polymers, large distributions of functional groups are present, with severely overlapping spectral bands. These NMR techniques have been shown to effectively separate many of the overlapping bands in ^{13}C spectra of organic matter, allowing not only for conclusive resonance identification[10,11] but also for accurate functional group quantification.[10] In the current work, several of these NMR techniques are applied to synthetic polymers for the first time.

3.2. ^{13}C DP NMR with Dipolar Dephasing and 10 kHz MAS. The dephasing of ^{13}C NMR signals based on the $^{13}C-^{1}H$ dipolar interaction has long been used in the identification of nonprotonated carbon sites in organic materials. At moderate MAS frequencies <10 kHz, proton decoupling is usually gated off (typically for ~ 40 μs) before signal acquisition to achieve this signal selection by C−H dephasing. However, at higher MAS speeds (≥ 10 kHz), the C−H interaction is partially refocused due to a rotational echo caused by sample spinning. For ^{13}C NMR experiments utilizing MAS frequencies of 10−20 kHz, Mao and Schmidt-Rohr[10] recently introduced a pulse sequence (Figure 1b) that achieves signal selection through C−H dipolar dephasing with coincident recoupling of the C−H interaction. For ^{13}C DP/MAS spectra acquired without dephasing (Figure 1a) and with dephasing (Figure 1b), signal refocusing and recoupling are obtained with a ^{13}C 180° pulse applied at the sample rotation period t_r after the ^{13}C 90° excitation pulse. A Hahn echo is produced at time $2t_r$, where signal acquisition is initiated. For ^{13}C DP/MAS NMR with C−H dipolar dephasing (Figure 1b), the ^{13}C 180° pulse is applied in the middle of a short delay t_{CH} (with duration close to t_r) in which C−H dipolar decoupling is off.

Three thermally aged polypropylene samples with different ^{13}C labeling were analyzed using the C−H dipolar dephasing technique (Figures 2 and 3). ^{13}C DP spectra were acquired at room temperature (294 K) with a 10 kHz MAS frequency, which is optimal in minimizing spinning sideband size and overlap with resonances attributed to oxidation-induced functional groups in polyolefins.[5,19] Two ^{13}C DP/MAS spectra were obtained for each PP sample: a reference spectrum acquired with the pulse sequence in Figure 1a and a C−H dipolar-dephased spectrum acquired with the sequence in Figure 1b. The signals of nonprotonated carbons and mobile segments are retained in C−H dipolar-dephased ^{13}C spectra.

Inspection of the main-chain PP resonances in Figure 2 demonstrates attenuation of signals from protonated carbons. The resonances of the tertiary (CH) carbons and the secondary (CH_2) carbons are clearly suppressed. Only small amounts of these main-chain carbon signals remain ($\sim$7% and $\sim$2% of the tertiary and secondary carbon signals, respectively), which can be readily seen in Figure 2, but appear more significant in Figure 3 in relation to the oxidation-induced functional group resonances, which are a few percent of the main-chain signals. This incomplete dephasing probably originates from highly mobile segments in the amorphous domains of the PP, where averaging of the C−H dipolar interaction is more significant. The methyl (CH_3) resonances are dephased by only $\sim$54% due to reduced C−H dipolar couplings from fast rotational jumps, which is commonly observed in experiments with dipolar dephasing.

The effect of C−H dipolar dephasing on the ^{13}C resonances attributed to oxidation-induced functional groups is shown in Figure 3. These resonances have been described and initially assigned to specific functional groups on the basis of isotropic chemical shifts in our previous NMR work.[5,6] The signals of the carbonyl (C═O) and carboxyl (COO) carbons in the range 160−220 ppm are all retained, consistent with their assignment to nonprotonated carbons. These results would exclude aldehydes and formate ester groups. On the basis of isotropic ^{13}C chemical shifts alone, the carbonyl resonances at $\sim$207 ppm (peak c in Figure 3) and $\sim$215 ppm (peak f) can be assigned[4] to chain-end methyl ketones and in-chain ketones, respectively, as discussed in our previous paper.[5] The carboxyl resonances (peaks d and e in Figure 3) can be identified with either carboxylic acid groups or ester/perester groups on the basis of their chemical shifts[5] and the C−H dipolar dephasing experiments. The signals attributed to tertiary hydroperoxides and/or dialkyl peroxides (85.3 ppm, peak a) and to tertiary alcohols (74.2 ppm, peak b) are partially dephased by 24%, although the carbons are nonprotonated. The dipolar coupling between the tertiary carbon and the hydroperoxy (OOH) or hydroxyl (OH) proton may be strong enough to induce this partial dephasing, as well as protons on the adjacent secondary CH_2 carbons, although these couplings would be intuitively weak. (Indeed, the C(2) carbonyl and carboxyl resonances showed

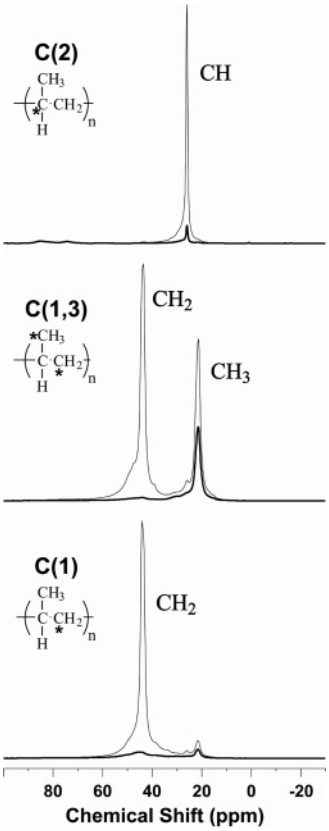

Figure 2. The 60 s ^{13}C DP/MAS spectra of selectively ^{13}C labeled polypropylene samples thermally aged in air, with emphasis on the main-chain carbons (tertiary CH, secondary CH_2, and methyl CH_3). Sample aging times and temperatures: C(2) labeled PP, 293 h at 80 °C; C(1,3) labeled PP, 319 days at 50 °C; C(1) labeled PP, 41 h at 110 °C. Two spectra acquired at room temperature (294 K) are shown for each labeled PP sample, a reference spectrum (thin line), acquired with the pulse sequence in Figure 1a, and a spectrum with the same number of scans and $^{13}C-^{1}H$ dipolar dephasing applied (thick line) according to the pulse sequence in Figure 1b. Dipolar dephasing retains nonprotonated carbon signals as well as the signals from methyl groups. A 10 kHz MAS frequency was employed in these experiments, which corresponds to a sample rotation period $t_r = 100$ μs (Figure 1a,b). In dipolar-dephasing experiments, a C−H dephasing delay $t_{CH} = 94$ μs (Figure 1b) was utilized.

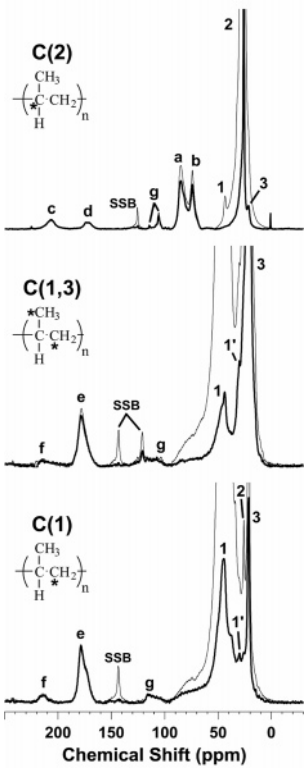

Figure 3. The same ^{13}C DP/MAS spectra presented in Figure 2, shown at 25× the maximum peak intensity of the reference spectra (thin lines) to emphasize the oxidation products. Major ^{13}C resonances are identified. Main-chain resonances: (1) secondary CH_2 carbon; (2) tertiary CH carbon; (3) methyl CH_3 carbon. Oxidation-induced functional group resonances: (a) tertiary hydroperoxides and/or dialkyl peroxides; (b) tertiary alcohols; (c) methyl ketones; (d) esters and/or peresters from the C(2) carbon; (e) esters and/or peresters from the C(1) carbon; (f) in-chain ketones; (g) hemiketals. The small peak labeled 1′ is most likely attributed to methyl groups formed from either the C(1) or C(3) carbons that are in chain-end tertiary alcohol or methyl ketone structures. Spinning sidebands of the main-chain resonances due to MAS at 10 kHz are designated with "SSB". The signals of nonprotonated carbons and carbons in mobile segments, particularly methyl groups, are retained in the C−H dipolar-dephased spectra (thick lines).

negligible dephasing, although protons on adjacent CH_2 carbons are in similar proximity. The carboxyl resonances, peaks d and e in Figure 3, are assigned to ester groups later in the paper.) Another source of this partial dephasing could be intramolecular hydrogen bonds, which have been observed in PP hydroperoxide groups by IR spectroscopy.[20]

Interestingly, the ^{13}C signals in the range 100−120 ppm (peaks g in Figure 3), which were assigned to vinylidene groups by other workers,[3,4] were retained in the dipolar-dephased spectra. This finding contradicts the protonated carbons in chain-end vinylidene groups (=CH_2) but does not exclude unsaturated, nonprotonated carbons. In our previous paper,[5] it was discussed that the second carbon in the double bond of the vinylidene group (and most unsaturated structures for that matter) should resonate in the range 135−155 ppm. The peak of this second carbon was not seen in the solution-state NMR spectra by previous workers.[3,4] Overlap with the strong solvent peaks in the same spectral region was cited as the reason for the lack of detection of this second peak. No resonance in the range of 135−155 ppm was observed in the C(2), C(1,3), or C(1) labeled sample spectra in our previous solid-state NMR studies,[5,6] in agreement with the current findings of the dipolar dephasing experiments.

The C−H dipolar dephasing also revealed a small peak near 30 ppm in the C(1) and C(1,3) labeled sample spectra. This peak is labeled 1′ in Figure 3 and is distinct from the main-chain tertiary carbon resonance (peak 2 in Figure 3) at 26 ppm. Although the resonance is identified with a protonated alkyl carbon on the basis of its chemical shift, it is retained after dipolar dephasing, which indicates segmental mobility. In our previous work,[5] we were able to identify methyl signals in oxidized C(1,3) samples, which were assigned to methyl groups in tertiary alcohol and chain-end methyl ketone structures on the basis of the isotropic chemical shift. Comparison of the C(1) and C(1,3) labeled sample spectra in Figure 3 shows the 1′ peak to be just as pronounced in the C(1) spectrum vs the C(1,3) spectrum. Hence, the 1′ peak could be attributed to mobile methyl carbons originating from the methylene C(1) carbon on the PP chain that are generated through chain cleavage as well as unreacted C(3) methyl carbons adjacent to oxidized C(2) carbons.

As shown in Scheme 1, PP chain cleavage is expected to occur through degradation of a tertiary hydroperoxide group (**1**) to yield an alkoxy radical (**2**), which in turns undergoes reaction to give a chain-end methyl ketone (**3**) and a free radical (**4**) centered on a C(1) carbon at the other chain end. (Note that the C(1), C(2), and C(3) carbons are accordingly labeled with Roman numerals I, II, and III in the scheme.) This reaction, which also generates the methyl ketone (**3**) and tertiary alcohol (**5**) groups, both of which have a C(3) methyl group as discussed above, has been widely described as a major step in the degradation of PP.[1,2] The chain-end C(1) radical (**4**) can further react by a number of routes. One expected route (shown in Scheme 1) would be termination by hydrogen abstraction from a neighboring chain, which is a favorable process because it results in conversion of a primary radical to a more stable tertiary

Scheme 1

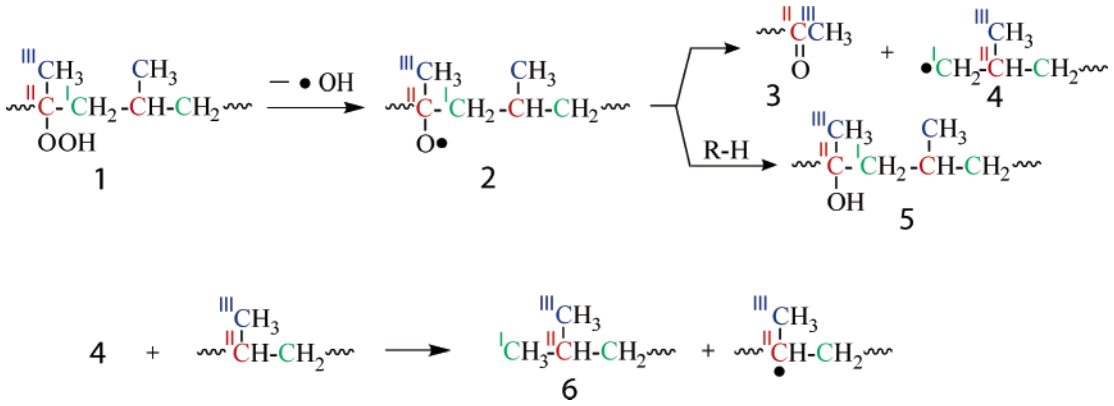

radical. This reaction yields a PP chain end (**6**) having both a C(1) and a C(3) methyl group. Hydrogen atom abstraction reactions between adjacent chains in solid-phase hydrocarbon materials have been documented previously.[21] The tertiary C(2) carbon near the chain end in **6** would be susceptible to further oxidation to form hydroperoxides, alcohols, and other chromaphores. Occurrence of further oxidation near chain ends formed during degradation is quite probable, given the localized nature of radical reactions expected within bulk polymers in the solid phase. Such oxidation products coming from **6** would give methyl signals having the chemical shift value and dipolar dephasing behavior that is observed for the 1′ peak in Figure 3.

3.3. DP/MAS with ^{13}C CSA Filtering. On the basis of the isotropic ^{13}C chemical shift, the resonances observed in the range 100−120 ppm (peaks g in Figure 3) could be assigned to either unsaturated structures (C═C), with sp^2-hybridized carbons, or to dioxygenated alkyl groups (O−C−O), with sp^3-hybridized central carbon sites. Such alkyl structures would include ketals and hemiketals, both with a nonprotonated central carbon, and acetals, with a protonated central carbon. (On the basis of the C−H dipolar dephasing results, acetals would be unlikely, as the resonances from 100−120 ppm are attributed to nonprotonated carbons.) The magnitude (frequency span) of the chemical shift anisotropy (CSA) of a specific carbon reflects the bonding symmetry about that carbon site.[22−24] For example, the CSA of an sp^3-hybridized alkyl carbon would be relatively small (full frequency span $\Delta\sigma$ < 70 ppm) because of its near tetrahedral bonding symmetry, whereas the CSA of an sp^2-hybridized unsaturated carbon would be much larger ($\Delta\sigma$ = 135−220 ppm) as a result of its planar bonding symmetry.[23] Indeed, the CSA magnitudes reported for ketals[23] and hemiketals[25] have been relatively small ($\Delta\sigma$ < 50 ppm).

Recently, Mao and Schmidt-Rohr[11] presented CSA-recoupling pulse sequences that suppress the ^{13}C NMR signals of sp^2- and sp-hybridized carbon sites while selecting the signals of sp^3-hybridized carbons. These CSA-filtering MAS experiments exploit the symmetry-based, systematic differences in the CSA magnitudes and rely on signal dephasing under the influence of the recoupled CSA. With a suitably chosen CSA-dephasing delay t_{CSA} (Figure 1c), the signals of carbons with large CSAs ($\Delta\sigma$ > 100 ppm), such as unsaturated and aromatic carbons, are almost completely dephased, whereas the signals of alkyl carbons are retained with >60% efficiency. The CSA-filtering experiments were originally used to separate dioxygenated alkyl bands from overlapping aromatic bands in the ^{13}C spectra of organic matter.[10,11] In the current study, the five-pulse CSA-filtering sequence[11] was utilized with ^{13}C DP/MAS (Figure 1c), using a CSA-dephasing delay t_{CSA} = 35 μs to select the various carbon signals.

The CSA-filtering technique was applied to a heavily degraded, C(2) labeled PP sample, as shown in Figure 4. A reference spectrum was acquired with a CSA-dephasing delay t_{CSA} = 3 μs, after which time little CSA dephasing has occurred. Signals from the main-chain tertiary (CH) carbon at 25.9 ppm have dephased by only 6%, which agrees very well with simulations by Mao and Schmidt-Rohr.[11] Likewise, the tertiary alcohol resonance at 74.2 ppm has dephased by 19%, which also is in good agreement with simulations. Signals from the carboxyl carbon resonating near 172 ppm have been completely suppressed, as expected for an sp^2-hybridized carbon site. Interestingly, the tertiary peroxide resonance at 85.3 ppm has dephased by 38%, which is similar behavior to a methoxy (OCH_3) carbon.[11] This increased dephasing would be caused by a ^{13}C CSA that is slightly larger ($\Delta\sigma$ > 60 ppm) than typical

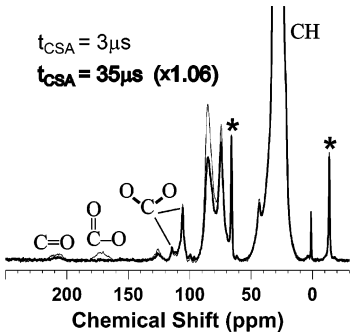

Figure 4. The 60 s ^{13}C DP/MAS spectra of a C(2) labeled polypropylene sample thermally aged 293 h in air at 80 °C, shown at 50× the maximum peak intensity. The spectra were acquired at room temperature (294 K) with a MAS frequency of 4 kHz using the five-pulse CSA-filtering sequence of Mao and Schmidt-Rohr[11] (Figure 1c), where t_{CSA} is the CSA-dephasing delay. A reference spectrum (thin line, t_{CSA} = 3 μs) and a CSA-filtered spectrum (thick line, t_{CSA} = 35 μs) are presented. The CSA-filtered spectrum is scaled by the factor shown (1.06). Spinning sidebands of the main-chain tertiary CH carbon due to MAS at 4 kHz are designated with an asterisk (*).

alkyl CSAs. However, no alkyl peroxide CSA measurements were found in the literature to verify this. The two small, reasonably narrow peaks at 105.7 and 114.1 ppm, which had been attributed to vinylidene groups by previous workers,[3,4] showed dephasing (6%) comparable to the main-chain tertiary carbon resonance. This finding would indicate the ^{13}C resonances from 100−120 ppm in the C(2) sample spectrum to be attributed to dioxygenated alkyl groups, specifically ketal groups and/or hemiketal groups, rather than sp^2-hybridized carbons from double bonds.

The CSA-filtering experiment can be sensitive to the sample temperature, as demonstrated with a highly aged C(1) labeled PP sample in Figure 5. At room temperature (294 K), the signals at ∼179 ppm which are attributed to carboxylate derivatives (e.g., carboxylic acids and esters) should be significantly dephased by the CSA filter because of the typically large CSA of a carboxyl carbon ($\Delta\sigma$ ∼ 140 ppm for a typical carboxylic acid and ∼150 ppm for a typical ester).[23] However, the 179 ppm resonance only dephased by 40%. The main-chain secondary carbon (CH_2) resonance at 43.5 ppm dephased by 16% at room temperature, in good agreement with simulated CSA dephasing curves.[11] As the measurement temperature of the PP sample is lowered below T_g ∼ 273 K, the signals of the carboxyl carbon are effectively suppressed by the CSA filter (Figure 5). This result would indicate sufficient mobility of the carboxylate-derivative functional group at room temperature to partially average the ^{13}C CSA, thereby reducing the magnitude of the CSA. Note also in Figure 5 that the spinning sidebands of the carboxylate resonance become apparent in the reference spectra as the temperature is decreased below 273 K, confirming that these carbons have a large CSA and are becoming less mobile at subambient temperatures. The signals from 100−120 ppm are not suppressed in the C(1) sample spectra (Figure 5) at all temperatures, indicating that these resonances, as in the C(2) sample spectra, are consistent with ketal and/or hemiketal groups. It is also interesting to note that the C(2) carbonyl resonance near 207 ppm (peak c in Figure 3), which is clearly attributed to chain-end methyl ketones based on its isotropic chemical shift, shows only partial dephasing in Figure 4. As with the C(1) carboxyl carbon at ∼179 ppm, the chain-end ketones could have sufficient segmental mobility to partially average the large carbonyl CSA.

3.4. ^{13}C CSA Line Shapes from 2D SUPER NMR. Just as the symmetry of bonding can directly influence the magnitude

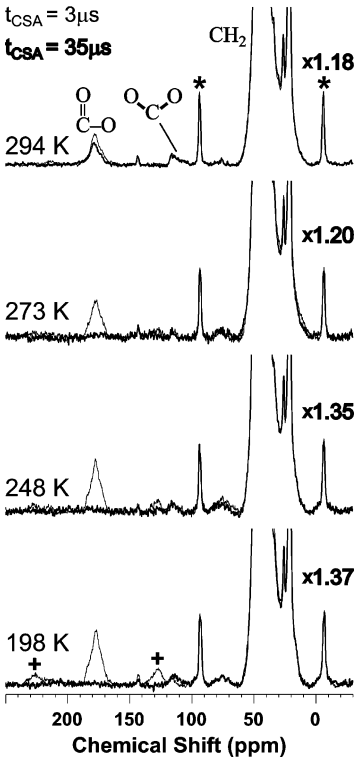

Figure 5. The 60 s ^{13}C DP/MAS spectra of a C(1) labeled PP sample thermally aged 41 h in air at 109 °C. The spectra were acquired at different temperatures (as shown in the figure) with a MAS frequency of 5 kHz. A CSA-filtered spectrum (thick line, $t_{CSA} = 35$ μs) and a reference spectrum (thin line, $t_{CSA} = 3$ μs) are presented for each measurement temperature. The CSA-filtered spectra are scaled by the factors given at the right of the figure. Spinning sidebands of the main-chain secondary CH_2 carbon and the carboxyl carbon resonating at ~179 ppm due to MAS at 5 kHz are designated with an asterisk (*) and a cross (+), respectively.

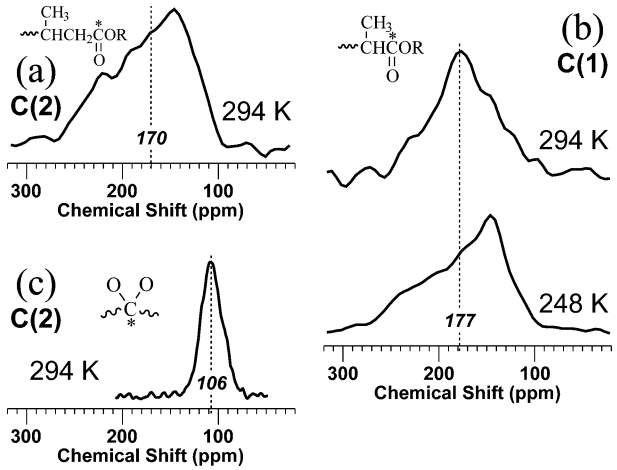

Figure 6. ^{13}C chemical shift anisotropy (CSA) powder patterns from 2D SUPER NMR spectra of selectively labeled polypropylene samples thermally aged in air. Sample aging times and temperatures: (a),(c) C(2) labeled PP, 293 h at 80 °C; (b) C(1) labeled PP, 41 h at 110 °C. SUPER spectra were acquired with the pulse sequence in Figure 1d at measurement temperatures shown in the figure. A CSA scaling factor $\chi' = 0.155$ was utilized. The CSA patterns were obtained as cross sections of the 2D SUPER spectra at the isotropic chemical shifts indicated in the figure with vertical dashed lines. The horizontal (ppm) scales were shifted to match the isotropic shifts correctly; no shearing was used in spectral processing. SUPER spectra of carboxylate esters (a and b) and ketals (c) were acquired with MAS frequencies of 5 and 2.5 kHz, respectively.

of the ^{13}C CSA, the local electronic structure of a carbon site can significantly affect the distinctive line shape of its CSA powder pattern.[22−24] For example, the carboxyl carbons (COO) of carboxylate derivatives, such as acids and esters, generally display large CSA magnitudes as a result of their sp^2-hybridization.[22,23] Hence, the CSA-filtering experiments described previously could not effectively distinguish the ^{13}C resonances of the various carboxylate derivatives, which have overlapping isotropic ^{13}C chemical shift ranges, particularly from 170−180 ppm (peaks d and e in Figure 3). However, the corresponding CSA line shapes of the carboxyl carbons can differ depending on the chemical structure of the specific carboxylate derivative group. The CSA line shapes of carboxylate esters (COOR) are systematically different from those of carboxylate (COO^-) and carboxylic acid (COOH) groups because of the replacement of the oxygen acid with an organic group R.[22,23] Ester CSAs are typically more symmetric, with small asymmetry parameters η and positive anisotropy parameters δ. As a result, the strong σ_{22} peak of the ester CSA powder pattern will generally occur upfield (to the right) on the chemical shift scale, whereas the σ_{22} peak of a typical acid CSA will be more central to the pattern, a chemical shift difference of >30 ppm.

Schmidt-Rohr and co-workers[13,18] have recently used the characteristic CSA line shapes of carboxyl carbons to assign resonances attributed to carboxylate derivatives in ^{13}C NMR spectra. To acquire these CSA powder patterns, 2D SUPER ^{13}C NMR[13] was utilized. This technique recouples the ^{13}C CSA under MAS during the evolution time t_1 (Figure 1d), separating quasi-static CSA patterns obtained in the indirect dimension ω_1 by isotropic ^{13}C chemical shifts in ω_2. The CSA patterns can then be potentially used in resonance assignments, molecular dynamics and orientation studies, and calculations of the CSA tensor.

In the current study, several specific ^{13}C resonances attributed to PP oxidation-induced functional groups were examined with the SUPER technique. Peaks d and e in Figure 3 are associated with nonprotonated C(2) and C(1) carboxyl carbons, respectively, and could be identified with either carboxylic acids or carboxylate esters. SUPER NMR would be useful in clarifying the assignments of these peaks, based on their corresponding CSA line shapes. Also, the CSA pattern (and in particular the CSA magnitude) of a resonance attributed to ketals and/or hemiketals would be of interest, especially in confirming the results of the CSA-filtering experiments discussed above.

2D SUPER spectra were acquired for heavily degraded C(1) and C(2) labeled PP samples, and CSA patterns were obtained as cross sections at specific isotropic chemical shifts (Figure 6). MAS frequencies of 2.5 and 5 kHz were used to obtain CSA patterns of dioxygenated alkyl (O−C−O) carbons and carboxyl (COO) carbons, respectively. Total sideband suppression (TOSS)[14] was applied before detection. TOSS increases the centerband to sideband intensity ratio under MAS, reducing distortions to the CSA line shape due to MAS frequencies smaller than half the CSA magnitude.[13]

The ^{13}C CSA powder patterns associated with peaks d and e in Figure 3 are presented in parts a and b of Figure 6, respectively. It is clear from the CSA pattern in Figure 6a that the C(2) carboxyl carbon resonating at 170 ppm is attributed to carboxylate ester (COOR) functional groups. The CSA line shape is symmetric, and the pronounced σ_{22} peak is upfield (to the right) of the isotropic chemical shift by ~25 ppm. Kinetic studies[5,6] have indicated that perester species partially contribute to this broad peak. Although no direct CSA measurements of peresters have been found in the literature, it is very possible that the CSA patterns of esters and peresters would have similar line shapes.

In the CSA-filtering experiments described earlier, it was hypothesized that the CSA of the C(1) carboxyl carbon resonating near 177 ppm (peak e in Figure 3) was temperature sensitive as a result of partial averaging induced by functional group mobility. This sensitivity was further probed with the SUPER technique (Figure 6b) at room temperature (294 K) and a subambient temperature (248 K) where effective suppression of the ^{13}C resonance by the CSA-filtering experiment was observed (Figure 5). The CSA patterns in Figure 6b confirm the results of the CSA-filtering experiments. At room temperature (294 K), the CSA pattern reveals partial isotropization, as indicated by the intensity peak at the isotropic chemical shift. However, at 248 K a CSA pattern exhibiting a symmetric line shape typical of a rigid carboxylate ester is clearly seen. The increased mobility of the C(1) ester group at room temperature could imply chain-end alkyl esters. Such functional groups could be the most stable solid-phase oxidation product forming from the further reaction of chain-end C(1) aldehydes and peracids, which were not detected in our NMR studies. In related GC-MS work,[8] we have found that CO_2 and CO gaseous products arising from the oxidative degradation of polypropylene predominantly originate from the methylene C(1) carbon on the PP chain, most likely from the reaction of unstable C(1) aldehydes and peracids. The C(1) ester may also be part of a larger chain-end γ-lactone structure. The occurrence of γ-lactones in PP oxidation has been discussed by previous workers.[26−28] However, the bulky nature of this end group would probably inhibit the structure from obtaining the room temperature mobility necessary to partially average the ester CSA.

The CSA powder pattern corresponding to the largest ketal resonance near 106 ppm in the C(2) labeled sample spectrum is shown in Figure 6c. The CSA has a relatively small magnitude ($\Delta\sigma \sim 48$ ppm), consistent with an sp^3-hybridized dioxygenated alkyl (O−C−O) structure. The SUPER results further confirm the assignment of the resonances in the range 100−120 ppm to ketal and/or hemiketal groups. Indeed, the estimated principal values derived from the CSA pattern in Figure 6c, $\sigma_{11} = 130 \pm 5$ ppm, $\sigma_{22} = 107 \pm 5$ ppm, and $\sigma_{33} = 82 \pm 5$ ppm, agree reasonably well with values recently reported by Iuliucci et al.[25] for a hemiketal structure in solid-phase erythromycin.

3.5. 2D HETCOR NMR. A highly aged C(2) labeled PP sample was analyzed with $^1H-^{13}C$ HETCOR NMR (Figure 7). Heteronuclear correlation (HETCOR) experiments between ^{13}C and ^1H under MAS conditions correlate the isotropic chemical shifts of these nuclei. The correlation NMR spectra give information about the protons in the environment of a specific carbon site. Frequency-switched Lee−Goldburg (FS-LG) homonuclear decoupling[15] was applied during the ^1H evolution (t_1) time to increase the resolution in the proton or indirect (ω_1) dimension. Lee−Goldburg cross-polarization (LG-CP)[16,17] of 0.5 ms duration was used to attenuate $^1H-^1H$ dipolar couplings and suppress ^1H spin diffusion during polarization transfer to ^{13}C. The LG-CP shows mostly one- and two-bond H−C through-space connections in the HETCOR spectrum.

The ^1H slices in Figure 7b reveal nearby protons at the major oxidized C(2) carbon sites. The main-chain tertiary carbon (CH) slice is presented as a reference. All of the oxidized C(2) carbon sites were found to be nonprotonated in the dipolar dephasing experiments discussed above. Hence, the correlated protons indicated by the slices in Figure 7b, with the exception of the reference CH slice, are "connected" through space to the carbon sites by approximately two bond lengths. All of the oxidized C(2) carbons show correlation with aliphatic protons, which resonate near 2 ppm. These aliphatic protons are most likely in backbone CH_2 groups that are adjacent to the C(2) carbon. Note the downfield (left) shift of the aliphatic protons correlating with the carbonyl carbon (C═O) of the methyl ketone structure because of increased deshielding caused by the carbonyl group.

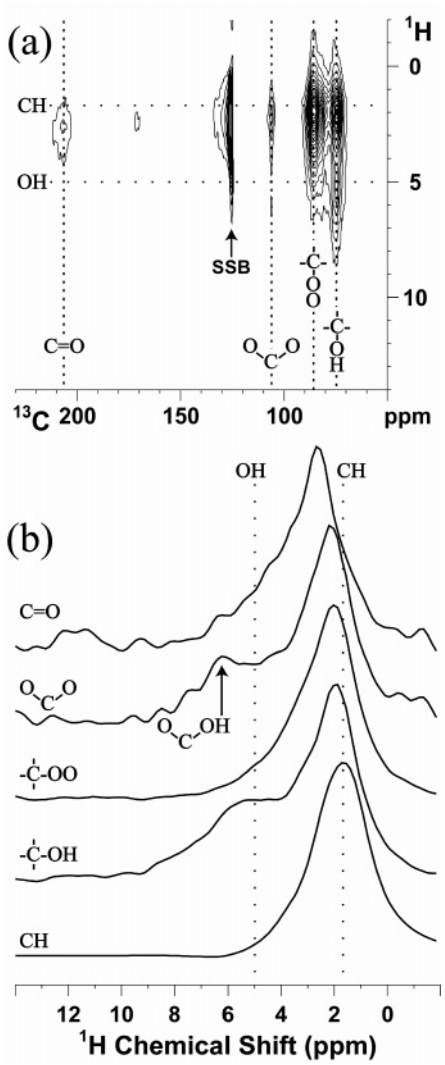

Figure 7. 2D $^1H-^{13}C$ HETCOR NMR spectrum of a C(2) labeled polypropylene sample thermally aged 293 h in air at 80 °C. The spectrum was acquired at room temperature (294 K) with a 10 kHz MAS frequency using FS-LG[15] homonuclear decoupling during the ^1H evolution and LG-CP[16,17] with a 0.5 ms contact time (see Figure 1e for pulse sequence). (a) 2D HETCOR spectrum, with emphasis on the oxidation-induced functional groups (>50 ppm in ^{13}C). The resonance labeled "SSB" is the spinning sideband of the main-chain tertiary (CH) carbon resonance due to MAS at 10 kHz. (b) ^1H slices at various isotropic ^{13}C chemical shifts: methyl ketone (C═O), 207 ppm; ketal (O−C−O), 106 ppm; tertiary peroxide (C−OO), 85 ppm; tertiary alcohol (C−OH), 74 ppm; main-chain tertiary (CH) carbon, 26 ppm. The hydroxyl (OH) proton in the hemiketal structure resonating near 6 ppm is indicated in the figure.

The only oxidized C(2) carbons showing any correlation to protons other than the aliphatic main-chain protons are the tertiary alcohol (C−OH) and ketal (O−C−O) groups. Both of these carbons are correlating with protons that resonate in the range 4−7 ppm, which correspond to hydroxyl (OH) protons. These isotropic ^1H chemical shifts are typical for hydroxyl groups in solid polymers,[29] where strong hydrogen bonds induce downfield (left) shifts. While the overall concentration of oxidized species in the PP materials is not large, the oxidation can be expected to be highly localized on a molecular scale because of free radical chain reactions taking place within the solid materials. NMR measurements on these samples, which

Scheme 2

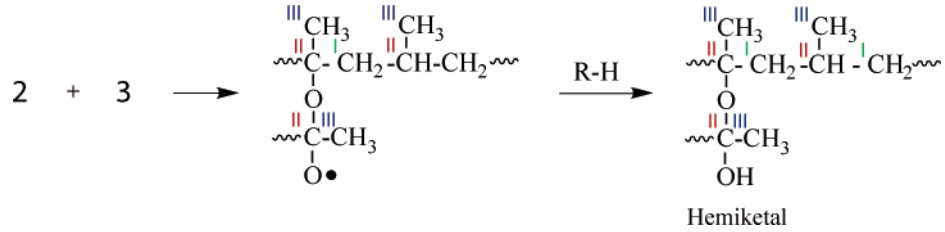

remain in their "undisturbed" solid-phase condition, most likely reflect elevated concentrations of hydroxyl and other polar groups within close proximity to each other, resulting in hydrogen bonds. Indeed, hydrogen bonding in PP hydroperoxides has been observed.[20]

The hydroxyl group attached to a ketal carbon (resonating near 106 ppm) is indicative of the presence of hemiketal structures. Because the other resonances in the range 100−120 ppm, which we assign to ketal functionalities, are relatively small and broad, it would be difficult to conduct the HETCOR experiment in a reasonable experiment time to determine whether they are also hemiketals.

3.6. Hemiketals in Oxidatively Degraded Polypropylene. This study has brought a collection of advanced solid-state NMR techniques to bear on elucidating the molecular structure underlying the peak intensity in the 100−120 ppm spectral region of oxidatively degraded PP. Only a few chemical species would resonate in this region of the ^{13}C NMR spectrum, and the most obvious assignment, double bonds due to olefins or aromatic groups, can be effectively ruled out by the results obtained here. Instead, the occurrence of ketal functionalities, and in particular the assignment of the 105.7 ppm resonance to hemiketal groups, as a significant product class not reported before in the oxidation of PP, is supported by multiple lines of evidence. A reasonable mechanism for formation of this functionality, proceeding through the primary free radical pathways operating in PP oxidation, is shown in Scheme 2. Methyl ketones (**3**), arising from a tertiary C(2) carbon atom (Scheme 1), have been described by many investigators as important PP degradation products, and indeed our previous NMR results on the isotopically labeled PP materials have identified significant quantities of C(2) methyl ketone groups.[5,6] The tertiary alkoxy radical (**2**) in Scheme 1 is considered an important and abundant reactive species in PP oxidation chemistry. Reaction of this radical with a methyl ketone group is envisioned to occur as shown in Scheme 2, resulting in another alkoxy radical that can then abstract a hydrogen atom to yield an OH group.

Oxygen-centered radicals (both alkoxy radicals and •OH) are known to add to C═C double bonds.[30] The addition of •OH to the C═O double bond of a ketone has been discussed before.[31,32]

Addition of an alkoxy radical (**2**) to an in-chain ketone in a process analogous to Scheme 2 would similarly yield a hemiketal. Our prior results[5,6] with the labeled PP materials have identified the presence of in-chain ketones, which originate from the C(1) carbon. This mechanism could thus underlie the formation of C(1) and C(2) ketals, both of which are found.[5,6]

Other mechanisms could be proposed to account for hemiketal formation, for example by the reaction of an alcohol with a ketone, which is a preparative route in organic synthesis and which requires catalysis by acid or base. However, while some acid or base may be present in the oxidizing PP matrix due to oxidation products, it may not be in sufficient concentration. Also problematic for this alternative mechanism is the fact that in the presence of high enough acid or base to catalyze the reaction the equilibrium concentration of product may be unfavorable.

4. Conclusions

Oxidation products in aged polypropylene samples with selective ^{13}C isotopic labeling have been identified with a suite of one- and two-dimensional solid-state ^{13}C NMR experiments. Several of these techniques have been recently developed and employed in the characterization of complex biosolids-derived and natural organic matter, and are applied here in the study of synthetic polymers for the first time. Using these techniques, several oxidation-induced functional groups, including carboxylate esters and ketal groups, have been identified by assignment of their corresponding resonances in ^{13}C NMR spectra. Hemiketal groups have been experimentally observed for the first time to our knowledge in oxidized polypropylene.

It was found that the NMR techniques which employ the ^{13}C CSA in resonance identification can be temperature sensitive as a result of molecular motion-induced averaging of the CSA. Decreasing the sample temperature to an appropriate, material-dependent level, thereby reducing the molecular mobility, can then allow such experiments to effectively identify chemical species.

This study further demonstrates the utility of selective isotopic labeling in the examination and elucidation of complex degradation mechanisms in polymers. The techniques utilized in this study would require intolerable experiment times for unlabeled materials. Also, the various ^{13}C resonances attributed to oxidation products would be severely overlapping, hindering efforts to identify product origin on the macromolecular chain. However, the combination of selective labeling and advanced NMR techniques permits detailed and comprehensive analyses of polymer oxidation chemistry.

Acknowledgment. Sandia is a multiprogram laboratory operated by Sandia Corporation, a Lockheed Martin Company, for the United States Department of Energy's National Nuclear Security Administration under Contract DE-AC04-94AL8500. The authors express their thanks to Sara Klamo and Prof. John Bercaw for providing the C(1) labeled PP material, to Robert Bernstein and Dora Derzon for sample preparation, to Greg Holland for assistance with the HETCOR experiment, to David Wheeler for insightful discussions concerning reaction mechanisms, and to Prof. Klaus Schmidt-Rohr for helpful discussions concerning the NMR experiments.

References and Notes

(1) Carlsson, D. J.; Wiles, D. M. *J. Macromol. Sci., Rev. Macromol. Chem.* **1976**, *C14*, 65−106.
(2) George, G. A.; Celina, M. Homogeneous and Heterogeneous Oxidation of Polypropylene. In *Handbook of Polymer Degradation*, 2nd ed.; Hamid, S. H., Ed.; Marcel Dekker: New York, 2000; pp 277−313.
(3) Busfield, W. K.; Hanna, J. V. *Polym. J.* **1991**, *23*, 1253−1263.
(4) Vaillant, D.; Lacoste, J.; Dauphin, G. *Polym. Degrad. Stab.* **1994**, *45*, 355−360.

(5) Mowery, D. M.; Assink, R. A.; Derzon, D. K.; Klamo, S. B.; Clough, R. L.; Bernstein, R. *Macromolecules* **2005**, *38*, 5035−5046.
(6) Mowery, D. M.; Assink, R. A.; Derzon, D. K.; Klamo, S. B.; Bernstein, R.; Clough, R. L. *Radiat. Phys. Chem.* **2007**, *76*, 864−878.
(7) Thornberg, S. M.; Bernstein, R.; Mowery, D. M.; Klamo, S. B.; Hochrein, J. M.; Brown, J. R.; Derzon, D. K.; Clough, R. L. *Macromolecules* **2006**, *39*, 5592−5594.
(8) Thornberg, S. M.; Bernstein, R.; Irwin, A. N.; Derzon, D. K.; Klamo, S. B.; Clough, R. L. *Polym. Degrad. Stab.* **2007**, *92*, 94−102.
(9) Bennett, A. E.; Rienstra, C. M.; Auger, M.; Lakshmi, K. V.; Griffin, R. G. *J. Chem. Phys.* **1995**, *103*, 6951−6958.
(10) Mao, J.-D.; Schmidt-Rohr, K. *Environ. Sci. Technol.* **2004**, *38*, 2680−2684.
(11) Mao, J.-D.; Schmidt-Rohr, K. *Solid State Nucl. Magn. Reson.* **2004**, *26*, 36−45.
(12) deAzevedo, E. R.; Hu, W.-G.; Bonagamba, T. J.; Schmidt-Rohr, K. *J. Chem. Phys.* **2000**, *112*, 8988−9001.
(13) Liu, S.-F.; Mao, J.-D.; Schmidt-Rohr, K. *J. Magn. Reson.* **2002**, *155*, 15−28.
(14) Dixon, W. T. *J. Chem. Phys.* **1982**, *77*, 1800−1809.
(15) van Rossum, B.-J.; Förster, H.; de Groot, H. J. M. *J. Magn. Reson.* **1997**, *124*, 516−519.
(16) van Rossum, B.-J.; de Groot, C. P.; Ladizhansky, V.; Vega, S.; de Groot, H. J. M. *J. Am. Chem. Soc.* **2000**, *122*, 3465−3472.
(17) Ladizhansky, V.; Vega, S. *J. Chem. Phys.* **2000**, *112*, 7158−7168.
(18) Mao, J.-D.; Hundal, L. S.; Schmidt-Rohr, K.; Thompson, M. L. *Environ. Sci. Technol.* **2003**, *37*, 1751−1757.
(19) Assink, R. A.; Celina, M.; Dunbar, T. D.; Alam, T. M.; Clough, R. L.; Gillen, K. T. *Macromolecules* **2000**, *33*, 4023−4029.
(20) Chien, J. C. W.; Vandenberg, E. J.; Jabloner, H. *J. Polym. Sci., Part A-1* **1968**, *6*, 381−392.
(21) Clough, R. L. *J. Chem. Phys.* **1987**, *87*, 1588−1595.
(22) Veeman, W. S. *Prog. Nucl. Magn. Reson. Spectrosc.* **1984**, *16*, 193−235.
(23) Duncan, T. M. *A Compilation of Chemical Shift Anisotropies;* The Farragut Press: Chicago, 1990.
(24) Schmidt-Rohr, K.; Spiess, H. W. *Multidimensional Solid-State NMR and Polymers;* Academic Press: San Diego, 1994.
(25) Iuliucci, R. J.; Clawson, J.; Hu, J. Z.; Solum, M. S.; Barich, D.; Grant, D. M.; Taylor, C. M. V. *Solid State Nucl. Magn. Reson.* **2003**, *24*, 23−38.
(26) Adams, J. H. *J. Polym. Sci., Part A-1* **1970**, *8*, 1077−1090.
(27) Iring, M.; Tüdös, F. *Prog. Polym. Sci.* **1990**, *15*, 217−262.
(28) George, G. A.; Celina, M.; Vassallo, A. M.; Cole-Clarke, P. A. *Polym. Degrad. Stab.* **1995**, *48*, 199−210.
(29) Horii, F.; Hu, S.; Deguchi, K.; Sugisawa, H.; Ohgi, H.; Sato, T. *Macromolecules* **1996**, *29*, 3330−3331.
(30) Kochi, J. K.; Oxygen Radicals. In *Free Radicals*; Kochi, J. K., Ed.; John Wiley & Sons: New York, 1973; Vol. 2, pp 665−710.
(31) Geuskens, G.; Kabamba, M. S. *Polym. Degrad. Stab.* **1982**, *4*, 69−76.
(32) Commereuc, S.; Vaillant, D.; Philippart, J. L.; Lacoste, J.; Lemaire, J.; Carlsson, D. J. *Polym. Degrad. Stab.* **1997**, *57*, 175−182.

MA062689J